Bioorganic & Medicinal Chemistry 17 (2009) 7789–7794

Contents lists available at ScienceDirect

Bioorganic & Medicinal Chemistry

journal homepage: www.elsevier.com/locate/bmc

Crystal structure of 3-isopropylmalate dehydrogenase in complex with NAD$^+$ and a designed inhibitor

Eriko Nango [a], Takashi Yamamoto [c], Takashi Kumasaka [b], Tadashi Eguchi [c,*]

[a] Department of Chemistry, Tokyo Institute of Technology, O-okayama, Meguro-ku, Tokyo 152-8551, Japan
[b] Japan Synchrotron Radiation Research Institute, 1-1-1, Kouto, Sayo-cho, Sayo-gun, Hyogo 679-5198, Japan
[c] Department of Chemistry and Materials Science, Tokyo Institute of Technology, O-okayama, Meguro-ku, Tokyo 152-8551, Japan

ARTICLE INFO

Article history:
Received 21 August 2009
Revised 12 September 2009
Accepted 15 September 2009
Available online 19 September 2009

Keywords:
Isopropylmalate dehydrogenase
β-Hydroxy acid oxidative decarboxylases
Leucine biosynthesis
Inhibitor
Crystal structure

ABSTRACT

Isopropylmalate dehydrogenase (IPMDH) is the third enzyme specific to leucine biosynthesis in microorganisms and plants, and catalyzes the oxidative decarboxylation of (2*R*,3*S*)-3-isopropylmalate to α-keto isocaproate using NAD$^+$ as an oxidizing agent. In this study, a thia-analogue of the substrate was designed and synthesized as an inhibitor for IPMDH. The analogue showed strong competitive inhibitory activity with K_i = 62 nM toward IPMDH derived from *Thermus thermophilus*. Moreover, the crystal structure of *T. thermophilus* IPMDH in a ternary complex with NAD$^+$ and the inhibitor has been determined at 2.8 Å resolution. The inhibitor exists as a decarboxylated product with an enol/enolate form in the active site. The product interacts with Arg 94, Asn 102, Ser 259, Glu 270, and a water molecule hydrogen-bonding with Arg 132. All interactions between the product and the enzyme were observed in the position associated with keto-enol tautomerization. This result implies that the tautomerization step of the thia-analogue during the IPMDH reaction is involved in the inhibition.

1. Introduction

Isopropylmalate dehydrogenase (IPMDH, EC1.1.1.85) is the third enzyme specific to leucine biosynthesis in microorganisms and plants.[1,2] The enzyme catalyzes the oxidative decarboxylation of (2*R*,3*S*)-3-isopropylmalate to α-ketoisocaproate using NAD$^+$ (Scheme 1) and requires a divalent metal ion, Mg^{2+} or Mn^{2+}, for its activity. IPMDH belongs to the family of β-hydroxy acid oxidative decarboxylases, which includes isocitrate dehydrogenase (ICDH)[3–5] and homoisocitrate dehydrogenase (Scheme 2a,b).[6,7] Tartrate dehydrogenase[8,9] and malic enzyme[10,11] are also classified in this family. With the exception of malic enzyme, all the enzymes in this family recognize each 2*R*-substrate that differs in the C3 substituent and are similar in sequence, structure, and catalytic mechanism. Although malic enzyme recognizes the (*S*)-hydroxy acid, L-malate, it is known that this enzyme catalyzes by a similar reaction mechanism.

Among various β-hydroxy acid oxidative decarboxylases, *Escherichia coli* ICDH (EcICDH) has been extensively investigated in regard to its catalytic mechanism and structure.[12–14] The crystal structures of wild-type EcICDH and its mutants have been elucidated in a quaternary complex of isocitrate or product, NADP$^+$ and metal ion.[12,13,15–18]

As to IPMDH, the crystal structures of IPMDH from *Thermus thermophilus*,[19,20] *Thiobacillus ferrooxidans*,[21] *Bacillus coagulans*,[22] *E. coli*,[23] and *Mycobacterium tuberculosis*[24] have been reported. However, the only complex structures reported to date are the binary complex of IPMDH from *T. thermophilus* (TtIPMDH) with NAD$^+$ and the structure of IPMDH from *T. ferrooxidans* (TfIPMDH) in the binary complex with the substrate, isopropylmalate.[20,21] The binary complex structure of TtIPMDH adopts a partially closed conformation in two domains, while apo-TtIPMDH has an open conformation. The results of small angle X-ray scattering analysis suggest that the ternary complex with a substrate and a cofactor adopts a fully closed conformation.[25] Compared with other β-hydroxy acid oxidative decarboxylases, there is only limited data available for the reaction mechanism of IPMDH, and information on the catalytic residues and other details are lacking. There is thus an immediate need for clarification of the structure of IPMDH in the complete complex with the substrate and NAD$^+$ in order to elucidate the mechanism of substrate recognition and the reaction mechanism.

In the present study, we report the design and synthesis of a sulfur-induced substrate analogue, (2*S*,3*S*)-(−)-3-methylmercaptomalic acid, as a potent inhibitor of TtIPMDH on the basis of the previous study designing and synthesizing for a homoisocitrate dehydrogenase inhibitor.[26] The resulting thia-analogue shows strong inhibition activity against TtIPMDH. Furthermore, we have determined the crystal structure of TtIPMDH complexed with the thia-analogue and NAD$^+$. The structure contained a decarboxylated product in the active site, which indicates that the tautomerization step of the thia-analogue during the IPMDH reaction is involved in the inhibition. Based on a comparison with the structure of TfIPMDH in complex

* Corresponding author. Tel./fax: +81 3 5734 2631.
E-mail address: eguchi@cms.titech.ac.jp (T. Eguchi).

0968-0896/$ - see front matter © 2009 Elsevier Ltd. All rights reserved.
doi:10.1016/j.bmc.2009.09.025

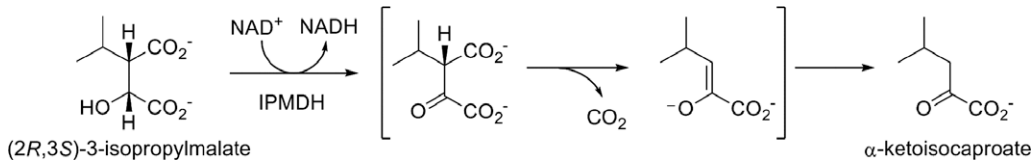

Scheme 1. Reaction catalyzed by IPMDH.

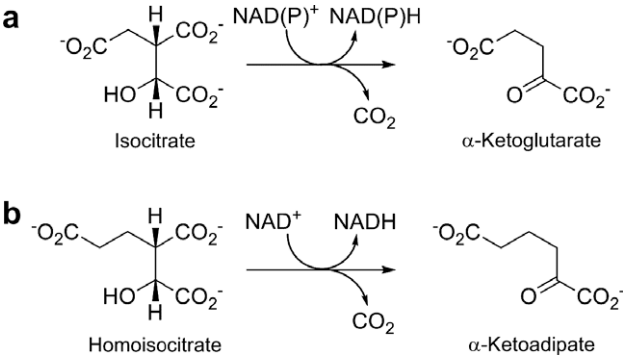

Scheme 2. Other β-hydroxy acid oxidative decarboxylases.

with isopropylmalate and the quaternary complex of ICDH, we also discuss the protein conformational change during the reaction and IPMDH reaction mechanism.

2. Results and discussion

2.1. Inhibitor design and synthesis

Various inhibitors of IPMDH have been developed by us and others.[27–36] In particular, *O*-isobutenyl and *O*-methyl oxalylhydroxamate were reported to be highly potent inhibitors against *Salmonella* IPMDH (K_i = 31 and 15 nM, respectively).[36] *O*-Isobutenyl oxalylhydroxamate exhibits herbicidal activity, since it inhibits the leucine biosynthesis in plants.[35] The hydroxamates could be deprotonated (because of the acidic amide NH group), and then the deprotonated form, which mimics the intermediary enolate of the IPMDH reaction, could be bound to the enzyme active site.

Recently, we reported a highly potent inhibitor, thiahomoisocitrate (Scheme 3a), for homoisocitrate dehydrogenase (HICDH) derived from *Saccharomyces cerevisiae*.[26] It is well known that substitution of a heteroatom such as sulfur and oxygen at the α-position of a ketone enhances the acidity of α-carbon and increases the stability of its enolate form.[37,38] Thus, the anticipated inhibition mechanism of the thia-substrate analogue was as follows: once the thia-substrate analogue has been accepted by HICDH and the enzyme reaction proceeds, the stability of the intermediary enolate (or enol) would be increased by hetero-atom substitution and the enolate intermediate might reside in the active site. This was found to be the case. Thiahomoisocitrate showed strong competitive inhibitory activity with K_i = 97 nM. The design for the tight-binding inhibition was accomplished by a rather simple substitution of homoisocitrate, so that we expected a similar replacement into isopropylmalate could yield a potential inhibitor of IPMDH.

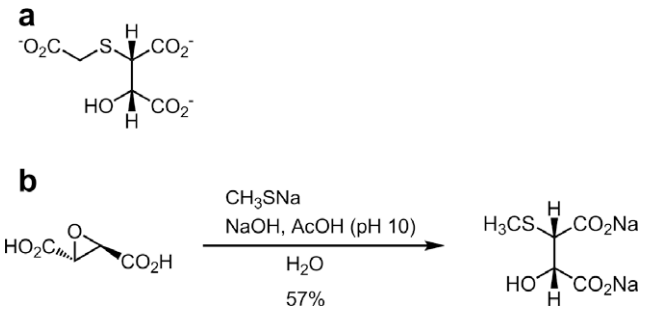

Scheme 3. Sulfur substituted analogues. (a) Thiahomoisocitrate. (b) Synthesis of (2*S*,3*S*)-(−)-3-methylmercaptomalate.

Based on this idea, we designed and synthesized (2*S*,3*S*)-(−)-3-methylmercaptomalate by introduction of a sulfur atom to the C3 position of malate as a potential inhibitor for IPMDH. Since IPMDH shows broad substrate specificity toward 3-alkylmalate, a thia-analogue was expected to be recognized by the enzyme. Thus, the thia-analogue was prepared by a similar method as in the case of thiahomoisocitrate, as shown in Scheme 3b. By this procedure, (2*S*,3*S*)-(−)-3-methylmercaptomalate was obtained in 57% yield from (2*R*,3*R*)-epoxysuccinic acid.

2.2. Inhibitory activity

The synthesized analogue was subjected to reaction with TtIPMDH as described previously.[28] The reactions were monitored by measuring the formation of NADH from NAD^+, and the kinetics was analyzed by a double-reciprocal plot. While the thia-analogue showed very low substrate activity, this compound was found to act as a strong competitive inhibitor (K_i = 62 nM), as anticipated. These results indicate that the thia-analogue binds to the active site, and the sulfur-substitute analogue is an effective inhibitor for β-hydroxy acid oxidative decarboxylases in general.

In order to elucidate the effect of other heteroatoms, we also synthesized and examined both the oxa-analogue and aza-analogue, but these analogues showed only moderate substrate activity and weak inhibition activity (data not shown). These results are well consistent with the fact that substitution by sulfur is known to be more effective for stabilization of enolate rather than oxygen and nitrogen.[38] Although similar inhibitors of isocitrate dehydrogenase, 3-mercapto-2-ketoglutarate, and 3-methylmercapto-2-ketoglutarate, have been achieved by heteroatom substitution, details of their inhibition mechanisms have not yet been discussed.[39]

These results strongly suggest that an enol/enolate intermediate during the IPMDH reaction is committed to this inhibition. In order to gain insights into the inhibition mechanism, we carried out a crystallization study of TtIPMDH in complex with the inhibitor and NAD^+.

2.3. Overall structure of the TtIPMDH–inhibitor–cofactor complex

It is known to be difficult to obtain a crystal of IPMDH in complex with a substrate and a cofactor,[25] since soaking with even substrate alone can easily break the TtIPMDH crystals. Indeed, we also attempted soaking experiments, but the crystal broke in the presence of a high concentration of the thia-analogue inhibitor (>150 μM). Thus, TtIPMDH was co-crystallized with the inhibitor, and NAD^+ and tetragonal crystals suitable for X-ray analysis were obtained by this method.

The X-ray structure of the ternary complex was solved by molecular replacement-phasing against data to 2.80 Å. The overall structure of the ternary complex is shown in Figure 1. The obtained ternary complex of TtIPMDH is a dimer of identical subunits that consists of two distinct domains, domain 1 and domain 2. Domain 1 is composed of four α helices, seven β strands, and a protruding arm-like region that forms the inter-subunit β sheet. Domain 2 contains seven α helices, five β strands, and both the N and C termini. As can be seen from the $2F_o - F_c$ density map in Figure 2, the inhibitor is bound in the cleft between domain 1 and domain 2 of both active sites of dimer. Interestingly, the inhibitor was converted into a decarboxylated compound by the enzyme reaction. Although an essential magnesium ion was added to the crystallization solution, no metal was found around the product in the active site.

The NADH molecule is located on the side of domain 2, which is the same position as that of NAD^+ in the TtIPMDH–NAD^+ complex.[20] The nicotinamide mononucleotide moiety of NADH in this ternary complex was disordered, and thus its structure could not be determined. In the previous report, although the nicotinamide ring of NAD^+ in the TtIPMDH–NAD^+ complex was assigned, it showed a high *B*-factor and its density was very weak. In addition, in the EcICDH quaternary complex analysis, the phosphate backbone and the nicotinamide ring of the $NADP^+$ molecule in the binary complex were unobservable, while the cofactor in the quaternary complex of isocitrate, $NADP^+$, and Ca^{2+} was well-ordered. Therefore, the cofactor would only be oriented appropriately in the presence of the substrate and the metal ion.

The structure of apo-TtIPMDH is known to adopt an open conformation,[19] while the TtIPMDH–NAD^+ complex structure shows a partially closed conformation (Fig. 1b). Although the ternary complex structure was expected to adopt a fully closed conformation by induced-fit,[25] it was found to exist in a partially closed conformation that is similar to the TtIPMDH–NAD^+ complex with an average root-mean-squared difference (rmsd) for 350 Cα atoms of 0.32 Å. However, the positions of residues 50–62, 77–99, and 306–316 are shifted in the ternary complex relative to their locations in the binary complex. In particular, both the main chain and side chain of residues 77–99, which interact with the nicotinamide ribose and the decarboxylated product, showed significant conformational change.

In this structure, no magnesium ion exists in the active site despite the fact that the ion is essential for the enzyme reaction, although the structures of other β-hydroxy acid oxidative decarboxylases in complex with a decarboxylated product contain a divalent ion.[43,44] After oxidative decarboxylation, the coordinated magnesium ion would be released while the formed stable enol product and NADH reside in the active site in the ternary complex. Thus, the decarboxylated enol product may not cause strong interaction with the magnesium ion. Consequently, it seems likely that when a cofactor, substrate, and divalent metal ion are bound in the active site, TtIPMDH adopts a closed conformation. After the magnesium ion release, the enzyme may not be able to keep a closed conformation. Therefore, a closed conformation of TtIPMDH may turn to a partially closed conformation, as observed in the present study.

Conformational change as a result of binding a product was observed in other β-hydroxy acid oxidative decarboxylases. In

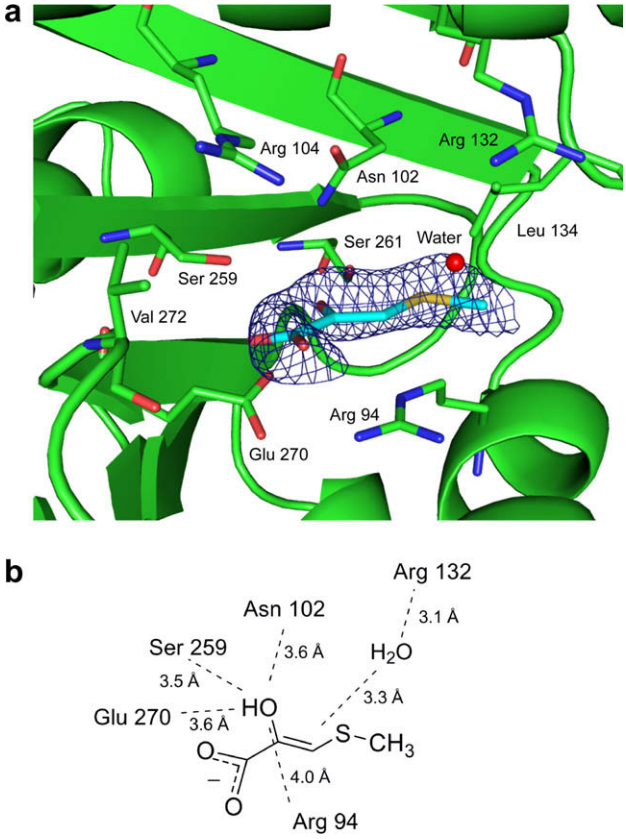

Figure 2. The decarboxylated product resulting from the inhibitor bound to TtIPMDH. (a) $2F_o - F_c$ Density map in the active site (contour level 1σ). The decarboxylated product is shown as a stick model, colored according to atom types (carbon cyan, oxygen red, and sulfur yellow). (b) Schematic drawing of the product-binding site.

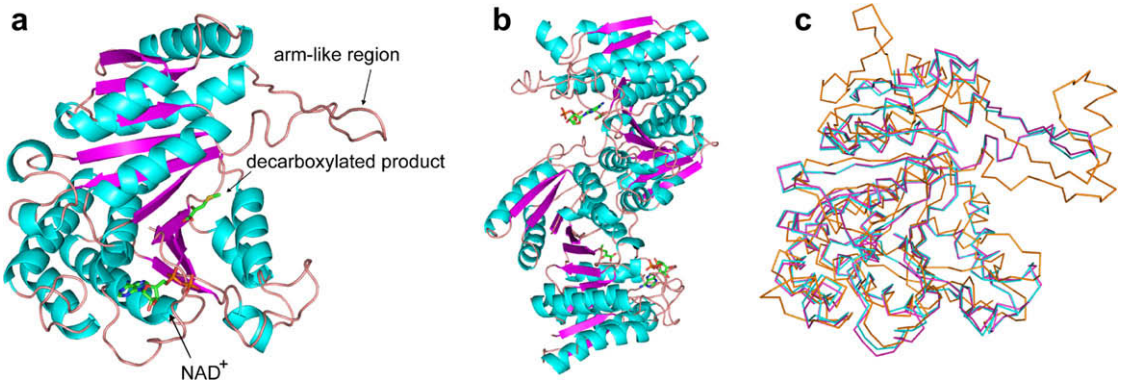

Figure 1. Overall structure of the TtIPMDH–inhibitor complex. (a) Schematic drawing of the monomer of the TtIPMDH–inhibitor complex. The β strands are shown in pink, α helices in cyan, and the connecting loops in light pink. The NAD^+ bound to the enzyme and the decarboxylated product in the active site are shown as stick models, colored according to the atom types (carbon green, oxygen red, nitrogen blue, sulfur yellow, and phosphorus orange). (b) Schematic drawing of the dimer of the enzyme. (c) Superimposition of the TtIPMDH ternary complex (cyan) onto the apo-TtIPMDH structure (pink, PDB entry 1IPD) and the quaternary complex of EcICDH (orange, PDB entry 1AI2).

EcICDH, while the apoenzyme can adopt both an open and a closed conformation, the complex structures with a substrate and/or a cofactor are in the closed form that is remarkably similar to that of the apoenzyme.[12,15,40–42] However, the complex which bound the decarboxylated product (α-ketoglutarate), Ca^{2+}, and NADPH showed a conformational change involved in the active side residue,[43] and thus it is clear that the conversion of the substrate to the product induces large movement.

2.4. Inhibitor binding site and inhibition mechanism

The decarboxylated product resulting from the inhibitor is located in the back of the cleft that is suggested to be the active site. It is found that the oxidation of the thia-analogue by NAD^+ proceeds and that the inhibition is caused by slow reaction after the decarboxylation, because the decarboxylated product resides in the specific site. The electron density of the decarboxylated product showed a planar shape. Thus, it seems likely that most of the product exists in the form of enol/enolate rather than the keto form (Fig. 2). The occupancy of the product was estimated to be 60%. However, as the inhibitor concentration in co-crystallization was increased in order to obtain higher occupancy, the resolution of crystal decreased, and thus we could not increase the concentration of the inhibitor to more than 1 mM.

The product-binding site is formed by Arg 94, Asn 102, Arg 104, Arg 132, Leu 134, Ser 259, Ser 261, Glu 270, and Val 272. Most of these residues are located within the van der Waals distance of the product. Interestingly, no residue forms a direct and strong hydrogen bond with the product despite the tight binding of the inhibitor. Only one water molecule is found at 3.3 Å apart from the α position of the product. Arg 132 is located in a position to bind this water molecule via weak hydrogen-bonding (Fig. 2b). Four residues, Arg 94, Asn 102, Ser 259, and Glu 270, interact with the enol/enolate oxygen atom of the product via weak hydrogen-bonding. Thus, the main interaction between the product and enzyme seems to be the van der Waals interaction. These interactions induce the formation of a product-binding pocket in the active site, thereby trapping the product.

All the observed interactions with the product seem to be involved in the keto-enol tautomerization, which implies that the tautomerization step of the decarboxylated product is due to the inhibition. This tautomerization step may be a very slow reaction, since the intermediary enol/enolate of the thia-analogue is stable. Although the product resides in this ternary complex structure, the inhibitor is not an irreversible inhibitor but a reversible inhibitor because it shows competitive inhibitory activity. Thus, the product could be slowly released from the active site. Further, the decarboxylated product might exist in the enol form rather than the enolate form because stabilization of the enolate form by electrostatic interaction or strong hydrogen-bonding interaction with the enzyme residue could not be observed except weak hydrogen-bonding.

Although the decarboxylated product resulting from the inhibitor was trapped in the active site without release, the product appears to move slightly to the back of the cleft compared with the position of isopropylmalate of the binary complex of TflPMDH,[21] as shown in Figure 3. On the other hand, in the EcICDH quaternary complex, α-ketoglutarate is located in nearly the same position as the substrate. γ-Carboxylate of α-ketoglutarate forms hydrogen-bonding interactions with Ser 113, and a metal ion is bound with the α-ketoglutarate carboxyl oxygen and α-carbonyl oxygen. However, in the ternary complex structure of TtIPMDH, the interaction between the product and residues is probably caused by a van der Waals interaction, and the strong interactions found in the EcICDH quaternary complex as mentioned above are absent. Thus, the product is likely to be located in a unique binding site that is slightly different from the original substrate-binding site.

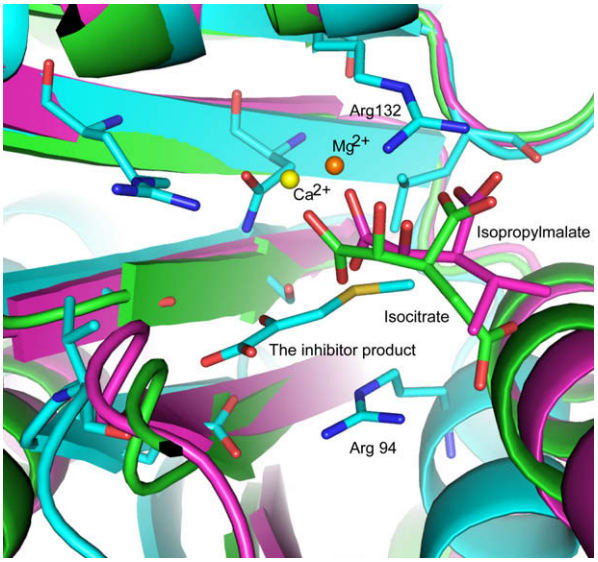

Figure 3. Superimposition of the TtIPMDH ternary complex active site residues (cyan) onto the binary complex of TflPMDH residues (pink, PDB entry 1A05) and onto the quaternary complex of EcICDH residues (green, PDB entry 1AI2). Magnesium ion (orange) is coordinated to isopropylmalate. Calcium ion (yellow) is coordinated to isocitrate.

All residues interacted with the product, Arg 94, Asn 102, Arg 132, Ser 259, and Glu 270, are conserved in IPMDHs from several origins. Given the active site of the ternary complex can be superimposed on that of the quaternary complex of EcICDH[15] and the binary complex of TflPMDH (Fig. 3), Arg 132 is firmly considered to recognize the C3 carboxylate of the substrate in the IPMDH reaction. Arg 94 may participate in the substrate recognition; however, Asn 102, Ser 259, and Glu 270 appear to be far away from the substrate. Although these residues may not act as a catalytic residue in the enzyme reaction directly, they could be involved in the delivery of a proton from catalytic residues.

3. Conclusions

The thia-analogue of a substrate, (2*S*,3*S*)-(−)-3-methylmercaptomalate, was designed and synthesized as a potential inhibitor for IPMDH. This compound showed strong competitive inhibitory activity toward TtIPMDH. We also determined the crystal structure of TtIPMDH in complex with the thia-analogue and NAD^+, which is the first example of a ternary complex structure of IPMDH. The structure showed a decarboxylated product in the active site, which indicated that the tautomerization step of the thia-analogue during the IPMDH reaction was involved in the inhibition.

Further, the structure including the decarboxylated product showed a partially closed conformation, which is slightly different from the binary complex structure with NAD^+ in the active site. Given the positional relationship between the product and catalytic residues, it is suggested that the enzyme reaction of TtIPMDH proceeds with conformational change step by step. These results should provide new insight into the reaction of IPMDH, and thus the development of this type of inhibitor may help to clarify the reaction mechanism of these enzymes.

4. Experimental

4.1. General

All chemicals were obtained commercially and used without further purification unless otherwise stated. (2*R*,3*R*)-Epoxysuccinic acid was purchased from Wako Chemicals. Dry CH_3CN were pre-

pared by distillation from P_2O_5. ^1H and ^{13}C NMR spectra were recorded on a JEOL LA-400 spectrometer. IR spectrum was recorded on a Horiba FT-710 Fourier-transform infrared spectrometer. Elemental analysis was performed with a Perkin–Elmer 2400 apparatus. Column chromatography was carried out with a Merck Kieselgel 60 (70–230 mesh; Merck). Enzyme reactions were monitored by measuring the NADH absorption at 340 nm on a Shimadzu UV-2450 UV–Vis recording spectrometer.

4.2. Synthesis of (2*S*,3*S*)-(−)-3-methylmercaptomalate

To a solution of (2*R*,3*R*)-epoxysuccinic acid (1.00 g, 7.57 mmol) in distilled water (21 ml) was added 3.0 M of aqueous sodium hydroxide until pH 7. Then, 15% solution of sodium methylthiolate (8.84 ml, 18.9 mmol) was added at 0 °C. Then, acetic acid was added until pH 10. The mixture was stirred for 10 h at 40 °C. The solution was evaporated and the residue was chromatographed over ion-exchanged resin (DEAE Sephadex A-20, 0–2.0 M formic acid). Recrystallization from acetonitrile gave (2*S*,3*S*)-(−)-3-methylmercaptomalate (780 mg, 57%): IR (KBr): 3498, 3430, 2856, 1693 cm^{-1}; mp 183 °C; ^1H NMR (D_2O) δ 4.47 (d, J = 6.0 Hz, 1H), 3.73 (d, J = 6.0 Hz, 1H), 2.10 (s, 3H); ^{13}C NMR (D_2O) δ 175.4, 173.7, 71.7, 52.1, 15.0; Anal. Calcd for $C_5H_8O_5S$: C, 33.33; H, 4.48; S, 17.80, Found: C, 33.57; H, 4.78; S, 18.00; $[\alpha]_D^{23}$ −54.0 (c 1.0, H_2O).

4.3. Inhibition assay

The thermophilic IPMDH derived from *T. thermophilus* HB8 (TtIPMDH) was prepared and purified as described previously.[45] Kinetic measurements were performed at 60 °C in an assay mixture (total 700 μl) containing 50 mM Hepes-NaOH (pH 7.8), 100 mM KCl, 5.0 mM $MgCl_2$, and 5.0 mM NAD^+. A reaction mixture including TtIPMDH (0.1 μg) and IPM (3.3–20 μM) or the alternative analogues was pre-incubated for ca. 3 min, and the reaction was started by addition of NAD^+ to the reaction mixture. The formation of NADH was measured at 340 nm for 10 s. Data were graphically analyzed by Lineweaver–Burk double-reciprocal plots, and the kinetic parameters were estimated by Hanes plots or Dixon plots.

4.4. Crystallization, data collection and molecular replacement

A solution of TtIPMDH was concentrated to 15 mg/ml in 5 mM Hepes-NaOH at pH 7.5. Co-crystallization of TtIPMDH, the thia-analogue inhibitor, and NAD^+ was performed by vapor diffusion using sitting drops of the crystallization solution at 20 °C. A 5-μl droplet of 15 mg/ml protein solution containing 1 mM of the inhibitor, 1 mM $MgSO_4$, and 2 mM NAD^+ was mixed with the same amount of reservoir solution (4.0 M sodium formate) and the mixture was equilibrated against 1 ml reservoir solution. Tetragonal crystals were obtained in 1–3 weeks. Prior to data collection, crystals were transferred to fresh drops containing reservoir solution supplemented with 1 mM inhibitor, 1 mM $MgSO_4$, 2 mM NAD^+, and 30% (v/v) PEG400 and flash-cryocooled by transfer directly into a cold stream of nitrogen gas (100 K). Diffraction data were collected on a Mar225 CCD detector at beamline BL26B2 (SPring-8, Japan) by using a mail-in data collection system with the approval of RIKEN (Proposal No. 20080020). Data were processed with the HKL-2000 processing suite.[46] The crystal belongs to space group $P6_122$ (a = 103.5 Å and c = 186.4 Å). The asymmetric unit contains one protein molecule and 69% solvent. The crystallographic statistics are given in Table 1. The ternary complex structure was solved by molecular replacement using MOLREP[47] with the TtIPMDH–NAD^+ complex (PDB entry 1HEX) as a search model. Model building and refinement were carried out with Coot[48] and REFMAC5.[47] The final models were refined to 2.79 Å with R_{work} and R_{free} values of 0.197 and 0.250, respectively. The final refinement statistics are given in Table 1. Molecular graphic figures were created using PyMOL.[49] The coordinates have been deposited in the Protein Data Bank (2ZTW).

Table 1
Summary of crystallographic statistics

	TtIPMDH complex
Data collection	
Wavelength (Å)	1.00
Resolution range (Å)	89.80–2.79
Observed reflections	270,793
Unique reflections	15,395
$I/\sigma(I)$	6.6
R_{merge} (%)[a]	12.1
Refinement	
Resolution range (Å)	89.80–2.79
R_{work} (%) (No. of reflections)	19.7 (14,551)
R_{free} (%) (No. of reflections)	25.0 (728)
Rmsd bond length (Å)/angle (°)	0.015/1.65
Average B-factors (Å^2)	33.7
Main chain	33.0
Side chain	34.4
Solvent	29.1
Ligands	33.2

[a] $R_{merge} = \Sigma_{hkl} \Sigma_i |I_i(hkl) - \langle I(hkl)\rangle| / \Sigma_{hkl} \Sigma i\, I_i(hkl)$, where is the ith intensity measurement of reflection hkl, including symmetry-related reflections, and $\langle I(hkl)\rangle$ is its average.

Acknowledgment

We thank Dr. Masaki Yamamoto for the collection of data at SPring-8 BL26B2 via the mail-in data collection system.

References and notes

1. Burns, R. O.; Umbarger, H. E.; Gross, S. R. *Biochemistry* **1963**, *2*, 1053.
2. Hsu, Y. P.; Kohlhaw, G. B. *J. Biol. Chem.* **1980**, *255*, 7255.
3. Kornberg, A.; Pricer, W. E., Jr. *J. Biol. Chem.* **1951**, *189*, 123.
4. Agosin, M.; Weinbach, E. C. *Biochim. Biophys. Acta* **1956**, *21*, 117.
5. Moyle, J. *Biochem. J.* **1956**, *63*, 552.
6. Strassman, M.; Ceci, L. N. *J. Biol. Chem.* **1965**, *240*, 4357.
7. Rowley. B.; Tucci, A. F. *Arch. Biochem. Eiophys.* **1970**, *141*, 499.
8. Kohn, L. D.; Packman, P. M.; Allen, R. H.; Jakoby, W. B. *J. Biol. Chem.* **1968**, *243*, 2479.
9. Giffhorn, F.; Kuhn, A. *J. Bacteriol.* **1983**, *155*, 281.
10. Ochoa, S.; Mehler, A. H.; Kornberg, A. *J. Biol. Chem.* **1948**, *174*, 979.
11. Kaufman, S.; Korkes, S.; Del Campillo, A. *J. Biol. Chem.* **1951**, *192*, 301.
12. Hurley, J. H.; Dean, A. M.; Koshland, D. E., Jr.; Stroud, R. M. *Biochemistry* **1991**, *30*, 8671.
13. Bolduc, J. M.; Dyer, D. H.; Scott, W. G.; Singer, P.; Sweet, R. M.; Koshland, D. E., Jr.; Stoddard, B. L. *Science* **1995**, *268*, 1312.
14. Dean, A. M.; Shiau, A. K.; Koshland, D. E., Jr. *Protein Sci.* **1996**, *5*, 341.
15. Stoddard, B. L.; Dean, A.; Koshland, D. E., Jr. *Biochemistry* **1993**, *32*, 9310.
16. Lee, M. E.; Dyer, D. H.; Klein, O. D.; Bolduc, J. M.; Stoddard, B. L.; Koshland, D. E., Jr. *Biochemistry* **1995**, *34*, 378.
17. Chen, R.; Greer, A. F.; Dean, A. M. *Eur. J. Biochem.* **1997**, *250*, 578.
18. Doyle, S. A.; Beernink, P. T.; Koshland, D. E., Jr. *Biochemistry* **2001**, *40*, 4234.
19. Imada, K.; Sato, M.; Tanaka, N.; Katsube, Y.; Matsuura, Y.; Oshima, T. *J. Mol. Biol.* **1991**, *222*, 725.
20. Hurley, J. H.; Dean, A. M. *Structure* **1994**, *2*, 1007.
21. Imada, K.; Inagaki, K.; Matsunami, H.; Kawaguchi, H.; Tanaka, H.; Tanaka, N.; Namba, K. *Structure* **1998**, *6*, 971.
22. Tsuchiya, D.; Sekiguchi, T.; Takenaka, A. *J. Biochem.* **1997**, *122*, 1092.
23. Wallon, G.; Kryger, G.; Lovett, S. T.; Oshima, T.; Ringe, D.; Petsko, G. A. *J. Mol. Biol.* **1997**, *266*, 1016.
24. Singh, R. K.; Kefala, G.; Janowski, R.; Mueller-Dieckmann, C.; von Kries, J. P.; Weiss, M. S. *J. Mol. Biol.* **2005**, *346*, 1.
25. Kadono, S.; Sakurai, M.; Moriyama, H.; Sato, M.; Hayashi, Y.; Oshima, T.; Tanaka, N. *J. Biochem.* **1995**, *118*, 745.
26. Yamamoto, T.; Eguchi, T. *Bioorg. Med. Chem.* **2008**, *16*, 3372.
27. Aoyama, T.; Eguchi, T.; Oshima, T.; Kakinuma, K. *J. Chem. Soc., Perkin Trans. 1* **1995**, 1905.
28. Chiba, A.; Aoyama, T.; Suzuki, R.; Eguchi, T.; Oshima, T.; Kakinuma, K. *J. Org. Chem.* **1999**, *64*, 6159.
29. Chiba, A.; Arai, N.; Eguchi, T.; Kakinuma, K. *Chem. Lett.* **1999**, *12*, 1313.
30. Chiba, A.; Eguchi, T.; Oshima, T.; Kakinuma, K. *Tetrahedron* **1997**, *53*, 3537.
31. Chiba, A.; Eguchi, T.; Oshima, T.; Kakinuma, K. *Tetrahedron* **1999**, *55*, 2927.

32. Pirrung, M. C.; Han, H.; Chen, J. *J. Org. Chem.* **1996**, *61*, 4527.
33. Pirrung, M. C.; Han, H.; Ludwig, R. T. *J. Org. Chem.* **1994**, *59*, 2430.
34. Terasawa, H.; Miyazaki, K.; Oshima, T.; Eguchi, T.; Kakinuma, K. *Biosci., Biotechnol., Biochem.* **1994**, *58*, 870.
35. Wittenbach, V. A.; Teaney, P. W.; Hanna, W. S.; Rayner, D. R.; Schloss, J. V. *Plant Physiol.* **1994**, *106*, 321.
36. Wittenbach, V. A.; Rayner, D. R.; Schloss, J. V. *Biosynth. Mol. Regulat. Amino Acids Plants* **1992**, *7*, 69.
37. Bernasconi, C. F.; Kittredge, K. W. *J. Org. Chem.* **1998**, *63*, 1944.
38. Bordwell, F. G.; Bares, J. E.; Bartmess, J. E.; Drucker, G. E.; Gerhold, J.; McCollum, G. J.; Van der Puy, M.; Vanier, N. R.; Matthews, W. S. *J. Org. Chem.* **1977**, *42*, 326.
39. Plaut, G. W. E.; Aogaichi, T.; Gabriel, J. L. *Arch. Biochem. Biophys.* **1986**, *245*, 114.
40. Hurley, J. H.; Dean, A. M.; Sohl, J. L.; Koshland, D. E., Jr.; Stroud, R. M. *Science* **1990**, *249*, 1012.
41. Hurley, J. H.; Dean, A. M.; Thorsness, P. E.; Koshland, D. E., Jr.; Stroud, R. M. *J. Biol. Chem.* **1990**, *265*, 3599.
42. Hurley, J. H.; Thorsness, P. E.; Ramalingam, V.; Helmers, N. H.; Koshland, D. E., Jr.; Stroud, R. M. *Proc. Natl. Acad. Sci. U.S.A.* **1989**, *86*, 8635.
43. Stoddard, B. L.; Koshland, D. E., Jr. *Biochemistry* **1993**, *32*, 9317.
44. Tao, X.; Yang, Z.; Tong, L. *Structure* **2003**, *11*, 1141.
45. Miyazaki, K.; Kakinuma, K.; Terasawa, H.; Oshima, T. *FEBS Lett.* **1993**, *332*, 35.
46. Otwinowski, Z.; Minor, W.; Charles, W. C, Jr. *Methods Enzymol*; Academic Press, 1997. pp 307–326.
47. Murshudov, G. N.; Vagin, A. A.; Lebedev, A.; Wilson, K. S.; Dodson, E. J. *Acta. Crystallogr., Sect. D* **1999**, *55*, 247.
48. Emsley, P.; Cowtan, K. *Acta. Crystallogr., Sect. D* **2004**, *60*, 2126.
49. DeLano, W. L. The PYMOL Molecular Graphic System. San Carlos, CA: DeLano Scientific LLC; 2002.